Tailoring Magnetic Dipole Emission with Plasmonic Split-Ring Resonators

Sven M. Hein* and Harald Giessen†

4th Physics Institute and Research Center SCoPE, Universität Stuttgart, Pfaffenwaldring 57, 70550 Stuttgart, Germany

(Received 19 November 2012; revised manuscript received 14 May 2013; published 10 July 2013)

We numerically explore the emission behavior of magnetic dipole emitters located next to resonant plasmonic split-ring resonators (SRRs), which are well known for their large magnetic moment at their fundamental resonance in the near infrared. Our results are compared to the situation for electric dipole emitters, where the SRR can be described by solely its electric dipole moment. We show that a similar approach in the case of magnetic dipole emitters is not sufficient, as the symmetry breaking due to the gap has to be taken into account. We demonstrate how retardation between the emitter and the SRR can be used as an additional degree of freedom to manipulate the emission spectrum. Our concept will pave the road towards efficient plasmonic antennas for magnetic dipole emitters.

DOI: 10.1103/PhysRevLett.111.026803 PACS numbers: 73.20.Mf, 78.20.Bh, 78.67.−n

Introduction.—Magnetic dipole transitions are usually several orders of magnitude weaker than electric dipole transitions [1], yet they are technologically very relevant, for example in Lanthanoide-ion-doped lasing media [2]. However, the radiative properties of photon emitters highly depend on their photonic environment, i.e., on the local density of states (LDOS), which was first analyzed by Purcell [3]. Because of the high electric and magnetic fields around a resonantly excited plasmonic nanostructure, such a structure strongly modifies the LDOS [4]. This can enhance as well as suppress both radiative and nonradiative decay rates, depending on the location and frequency of the emitter. These effects have been used to differentiate between electric and magnetic transitions in Eu^{3+} ions, using a planar gold mirror [5] or other one-dimensional geometries [6]. The LDOS of *electric* dipole emitters has been thoroughly studied in the vicinity of different complex nanostructures [7–14]. Recently, decay rates of magnetic dipole [15] and even electric quadrupole transitions [16] were shown to be strongly modified by plasmonic scatterers. Since in all of these cases resonantly excited nanostructures transfer radiation from deep subwavelength objects into the far field, the notion of a "nanoantenna" has been coined to demonstrate this strong similarity to usual antennas [17,18]. However, for nanostructures, large nonradiative losses continue to be a challenge in the design of efficient nanoantennas, especially as soon as higher-order modes are excited, an issue which may also be tackled by using dielectric nanoantennas [19–22].

For magnetic dipole emitters, a promising candidate for a suitable antenna is a split-ring resonator (SRR), since it will couple very well to the emitter through its strong magnetic fields, especially at its fundamental resonance. We show in this Letter that resonantly excited SRRs are indeed able to enhance spontaneous decay rates by several orders of magnitude. Remarkably, the amount of power transferred to the far-field may reach its maximum at frequencies below or above the antenna resonance frequency, depending on the position of the emitter.

Environment dependence of emitter properties.—The decay rate γ of an emitter is commonly described by Fermi's golden rule [23]

$$\gamma = \frac{2\pi}{\hbar^2}\sum_f |\langle f|H_I|i\rangle|^2 \delta(\omega_i - \omega_f) \tag{1}$$

with the initial state $|i\rangle$, the final state $|f\rangle$, and the interaction Hamiltonian H_I, which can be written as

$$H_I = -\boldsymbol{p}\cdot\boldsymbol{E} - \boldsymbol{\mu}\cdot\boldsymbol{B} - \ldots \tag{2}$$

where the dots represent further higher order interactions, such as electric quadrupole terms. $\boldsymbol{p}$ is the electric and $\boldsymbol{\mu}$ the magnetic dipole moment of the emitter.

In order to differentiate between intrinsic emitter properties and the influence of the photonic environment on the decay rate, it is convenient to rewrite Eq. (1) as [23]

$$\gamma = \frac{\pi\omega}{3\hbar}(\varepsilon_0^{-1}|\boldsymbol{p}|^2\rho_E(\boldsymbol{r},\omega) + \mu_0|\boldsymbol{\mu}|^2\rho_B(\boldsymbol{r},\omega)), \tag{3}$$

where $\rho_{E,B}$ is the electric or magnetic LDOS, which gives the amount of phase space available for the emitted photon. The LDOS is proportional to the amount of power an oscillating dipole loses when it is placed at the respective position, which can be calculated via

$$P = (\omega/2)\lim_{\boldsymbol{r}'\to\boldsymbol{r}}[\mathrm{Im}(\boldsymbol{\mu}^*\overleftrightarrow{\boldsymbol{G}}_m(\boldsymbol{r},\boldsymbol{r}')\boldsymbol{\mu})] \tag{4}$$

for the case of magnetic dipole emitters, where $\overleftrightarrow{\boldsymbol{G}}_m(\boldsymbol{r},\boldsymbol{r}')$ is the magnetic dyadic Green's tensor [24] that gives the magnetic field $\boldsymbol{B}(\boldsymbol{r})$ of a magnetic dipole located at $\boldsymbol{r}'$. In order to calculate the Purcell factor, which describes the ratio of the decay rate γ to the decay rate in vacuum γ_0, one has to normalize P by the power P_0 the dipole would emit in vacuum. This Purcell factor correctly includes radiative

as well as nonradiative decay channels, in contrast to other definitions that use the mode volume [25].

Our model system.—In this Letter, we use an SRR made from gold to modify the photonic environment around the emitter. The dimensions of the SRR are given in Fig. 1. We numerically analyze our system using a discrete dipole approximation (DDA) which we implemented based on Ref. [26]. For the polarizability of the single dipoles, we use the Clausius-Mossotti relation with a dipole volume of 64 nm^3 and directly solve the linear equation that arises for the single polarizabilities in the DDA. Although the numerical accuracy of the DDA is known to be less than optimal [26] at this level of discretization, the overall physics is still well reproduced [27]. For gold we use a Drude model with the parameters given in [28], which is a fit to the data of Johnson and Christy [29]. The structure is placed in vacuum. The fundamental resonance is located at about 165 THz.

The fundamental plasmonic resonance of SRRs is well known for its high electric dipole moment in the gap as well as its high magnetic moment, which is generated by the circular current in the ring (see Fig. 1). Often, the properties of an SRR are successfully described by reducing it to these two dipole moments [30]. We will show to what extent this model is also able to correctly predict the coupling of dipole emitters to an SRR. While in other plasmonic structures high magnetic fields often coincide with dark modes, in the case of SRRs, the electric dipole moment renders the fundamental plasmonic resonance bright. This makes it especially suitable as a "magnetic nanoantenna."

Nevertheless, any resonantly excited plasmonic structure only reradiates a fraction of the stored energy into the far field; a substantial amount will be absorbed due to Ohmic losses. Therefore, one has to distinguish between a radiative decay rate γ_r and a nonradiative decay rate γ_{nr} of the emitter next to the structure. The power which is absorbed in the structure can be calculated in the DDA approach via [31]

$$P_{abs} = (\omega/2)\sum_i \left[\left(-\mathrm{Im}(\alpha_i^{-1}) - \frac{2}{3}k^3\right)|\boldsymbol{p}_i|^2\right]. \quad (5)$$

In this formula, α_i and $\boldsymbol{p}_i$ are the polarizability and the dipole moment of the ith dipole in the DDA. In order to obtain the power radiated into the far field P_{rad}, we subtract this quantity from the total power P emitted by the dipole [Eq. (4)]:

$$P_{rad} = P - P_{abs}. \quad (6)$$

Decay rate modification.—We first calculate the Purcell factor around an SRR for magnetic as well as, for comparison, electric dipole emitters (see Fig. 2). The decay rate is enhanced up to 4 orders of magnitude and resembles the absolute square values of the magnetic and electric field component in the direction of the emitter, $|E_x|^2$ and $|B_z|^2$. For the x-polarized electric emitter, we observe the typical intensity distribution we would also obtain, at least qualitatively, if we replaced the SRR by an electric point dipole [Fig. 2(a)]. The four dents at about $|x| = 50$ nm are sometimes referred to as "magic angles," especially in nuclear magnetic resonance [32], and are also a typical feature of a dipolar field distribution. They mark the locations at which a dipole exhibits no field component along the axis of its orientation. For these reasons we can qualitatively describe the coupling to an electric dipole emitter perfectly in terms of the coupling of the two electric moments.

If the interaction with a magnetic dipole emitter [Fig. 2(b)] was solely mediated by the magnetic dipole moment of the SRR, one would expect a circularly symmetric distribution since the magnetic moment of the SRR is pointing out of the drawing plane. This, however, is not the case. Two dents are clearly visible at the end of the "arms" of the SRR, which mark positions where the z component of the $\boldsymbol{B}$ field changes sign. This sign change is obviously caused by the symmetry breaking due to the gap.

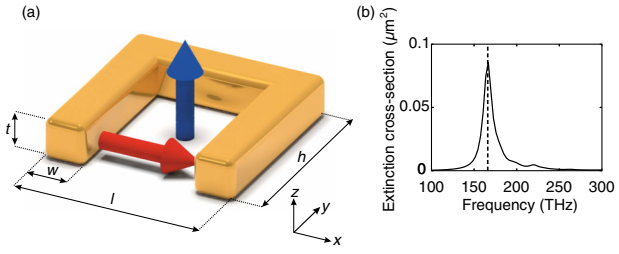

FIG. 1 (color online). The fundamental resonance of an SRR is often characterized by its electric dipole moment $\boldsymbol{p}$ (symbolized by the horizontal red arrow), which is oriented along the gap, and its perpendicular magnetic dipole moment $\boldsymbol{\mu}$ (vertical blue arrow) oriented along z. The dimensions of the SRR analyzed in this Letter are $l = h = 100$ nm; $w = t = 20$ nm. (b) shows the calculated extinction cross section for an x-polarized plane wave travelling along z, which shows a resonance at 165 THz, marked by the dashed line.

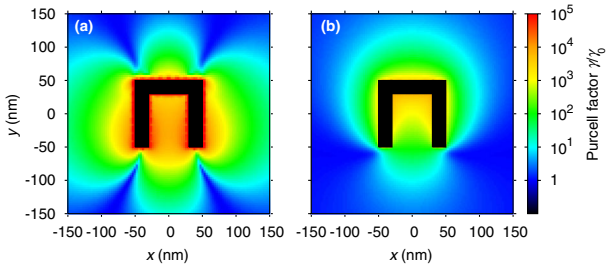

FIG. 2 (color online). Purcell factors around the SRR at its resonance frequency, for (a) electric dipole emitters oriented along the x axis, (b) magnetic dipole emitters oriented along the z axis. The enhancement of the LDOS and therefore the increase of the decay rate is several orders of magnitude in the direct vicinity of the structure and largely resembles the distribution of $|E_x|^2$ and $|B_z|^2$.

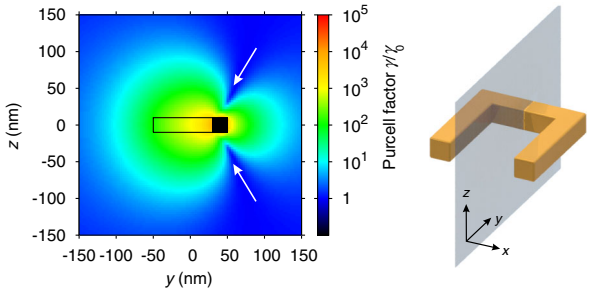

FIG. 3 (color online). Purcell factors in the x-z plane around the SRR at its resonance frequency for magnetic dipole emitters oriented along the z axis. The open rectangle shows the position of the arms of the SRR which lie above and below the plotted plane. In contrast to what one would expect from a magnetic dipole, the magic angles (white arrows), which are positions where the interaction vanishes, appear only on one side of the SRR.

The effects of this symmetry breaking are even more visible when we change the plane in which we plot the Purcell factor (Fig. 3). We only observe the magic angle near the cross bar of the SRR but not on the left side. This is a clear deviation from the pattern of an ordinary magnetic dipole, since the sign of the z component of $\boldsymbol{B}$ only changes *once* when we go halfway around the SRR in the upper or lower half-space, instead of changing *twice*. This sign difference matters especially when interference effects are investigated, in particular in the calculation of the radiative decay rate.

Far-field scattering and radiative decay rate.—In a first approximation, the change in the radiative decay rate and therefore the change of the power transferred to the far field can be calculated as [33]

$$\frac{\gamma_{\mathrm{rad}}}{\gamma_0} = \frac{P_{\mathrm{rad}}}{P_0} \approx \frac{|\boldsymbol{\mu} + \boldsymbol{\mu}_{\mathrm{ind}}|^2}{|\boldsymbol{\mu}|^2} \tag{7}$$

where $\boldsymbol{\mu}_{\mathrm{ind}}$ is the dipole moment induced in the SRR. The line shape of the radiative decay rate depends on the strength of the coupling to the SRR. We have to distinguish three regimes: For strong coupling, i.e., $\boldsymbol{\mu}_{\mathrm{ind}}$ is larger than the dipole moment $\boldsymbol{\mu}$ of the emitter itself, virtually all power emitted is scattered by the SRR. Therefore, we expect a Lorentzian peak in γ_{rad} around the plasmonic resonance of the SRR. This happens if the emitter is placed in the center of the SRR (cf. Fig. 4).

As soon as the coupling becomes weaker, e.g., for emitters placed outside the gap, the power radiated from the emitter *without* being scattered at the SRR may no longer be neglected, since these fields are of the same order of magnitude as the scattered fields. Therefore, one has to take the superposition of the fields of the emitter and the nanostructure into account, which strongly depends on the phase between them.

The third regime finally appears as soon as retardation plays a role, which will be analyzed later. We calculate the power transferred to the far field for an emitter displaced

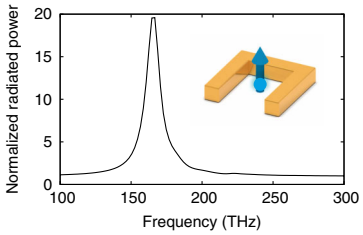

FIG. 4 (color online). Power transferred into the far field from a magnetic dipole emitter placed in the center of the SRR. The result is averaged over all possible orientations of the emitter and normalized to the power emitted in vacuum. We observe a large enhancement of more than 1 order of magnitude at the resonance, which exhibits a Lorentzian line shape.

from the SRR 100 nm along the x axis as well as along the y axis, using Eq. (6). The results for magnetic as well as for electric dipole emitters are shown in Fig. 5. Since the phase of the charge oscillation in the SRR and therefore the interference pattern with the unscattered light changes when the excitation frequency is tuned through the resonance of the SRR, the maximum of the radiative decay rate is detuned from the resonance frequency [34]. This explains the Fano-like resonance peaks in the emission spectra, since constructive interference leads to an increase and destructive interference to a decrease of γ_{rad}.

In the case of electric emitters [Figs. 5(a) and 5(b)], the results can easily be explained by a quasistatic model in which the electric emitter couples to the electric dipole moment of the SRR: For x-displacement (a), the parallel configuration is associated with lower energy. Since two parallelly aligned dipoles interfere constructively, the enhancement of the radiative decay rate also appears at lower frequencies, while above the resonance frequency, γ_{rad} is suppressed due to destructive interference. For y

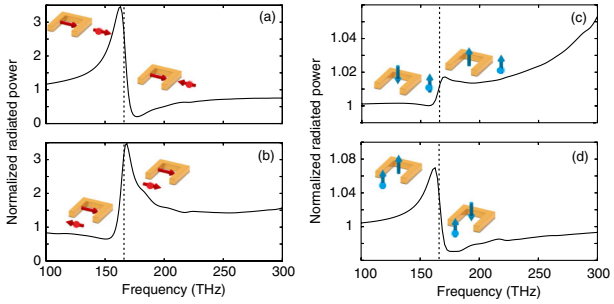

FIG. 5 (color online). Power transferred into the far field from electric [(a), (b)] and magnetic [(c), (d)] dipole emitters at different locations. The emitter is displaced 100 nm from the center of the SRR along the x axis [(a), (c)] and along the y axis in the direction of the gap [(b), (d)]. The dotted line marks the position of the fundamental plasmonic resonance. The results are averaged over all possible orientations of the emitter dipole moment. Thick arrows mark the dipole moments of emitter and SRR that give the dominant contribution.

displacement, the situation is reversed, since now the parallel configuration is of higher energy.

Applying the same quasistatic model to magnetic coupling would predict qualitatively similar spectra for displacements along the x and y axis, since the magnetic moment of the SRR is pointing along z. Figures 5(c) and 5(d) show that this is not the case. For displacements along the x axis, the quasistatic picture predicts a suppression below the resonance, since the antiparallel configuration is energetically favored. This is also what the simulation shows, however obscured by an overall increase for higher frequencies, which can be attributed to the second plasmonic resonance of the SRR.

For y displacements, the situation differs: The enhancement, i.e., the parallel configuration, appears at lower frequencies. This can be understood by inspecting the orientation of the magnetic field around an SRR: Near the gap, the z component of the magnetic field is oriented parallel to the magnetic dipole moment of the SRR, while for a perfect magnetic dipole, it would be antiparallel. This energetically favors the parallel orientation of the emitter, and therefore causes the maximum transmitted power to be situated *below* the resonance frequency.

We can still describe this behavior by the two-dipole model of the SRR, but only if we go beyond the quasistatic approximation and take the magnetic field of the *electric* dipole moment into account as well. In the gap region of any SRR, the magnetic field of the induced electric moment points opposite to the magnetic field of the induced magnetic moment. As shown in Fig. 5(d), the coupling to the electric dipole moment excedes the coupling to the magnetic dipole moment at this point. In the case of x displacement considered in Fig. 5(c), there is no magnetic field from the electric dipole moment; hence, we observe the bare coupling to the magnetic dipole moment. We would like to point out that also in the case of *electric* emitters there is a cross coupling to the *magnetic* dipole moment for symmetry reasons [30]; however, it appears to be small enough compared to the coupling to the electric dipole moment to be neglected in the explanation.

Coupling at larger distances.—We can further modify the line shape of the radiative decay rate by enlarging the distance between the SRR and the emitter. There are two major effects which contribute in this case. First, the interference pattern of two dipoles at distances of the order of a wavelength strongly differs from the interference of two close dipoles, and second, the phase between the SRR and the emitter may also be modified due to the retarded coupling [35]. We simulated a situation analogous to the situation depicted in Fig. 5, but this time with distances of 900 nm as well as 1000 nm, which is around $\lambda/2$ at the resonance frequency (cf. Fig. 6). Except for magnetic emitters displaced along the x axis, where the signal is too weak to be observed, the spectra are reversed compared to the displacement of 100 nm (Fig. 5). Since the phase

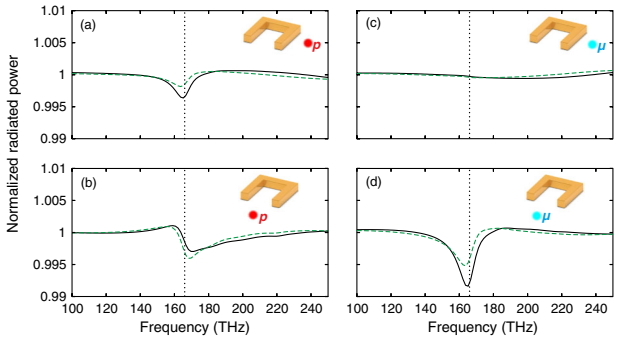

FIG. 6 (color online). Power transferred into the far field from electric [(a), (b)] and magnetic [(c), (d)] dipole emitters at different locations. The emitter is displaced 900 nm (black solid line) resp. 1000 nm (green dashed line) from the center of the SRR along the x axis [(a), (c)] resp. along the y axis in the direction of the gap [(b), (d)]. The dotted black line marks the position of the fundamental plasmonic resonance. The results are averaged over all possible orientations of the emitter dipole moment.

of a dipole changes only slightly up to distances of $\lambda/2$ due to the strong near fields, the effect is caused by the change in the interference pattern for dipoles at different separations. While two symmetrically oscillating dipoles are bright at close distances, they become dark at $\lambda/2$ separation and vice versa. Introducing retardation therefore offers a further degree of freedom to tune the behavior of dipole emitters. However, since the interaction strength decreases rapidly with increasing distance, the effects also become quite small.

Conclusion.—We found that SRRs are able to tremendously enhance the total decay rate of magnetic dipole emitters, making them a suitable tool to manipulate magnetic transitions. The radiative decay rate, however, crucially depends on the phase between the emitter and the plasmonic resonance. We were able to show that this leads to Fano-type spectra with enhancement as well as suppression of γ_r. The detuning of the maximal radiative decay rate from the plasmon resonance frequency is location dependent. While in the case of electric dipole emitters we explained this behavior by the quasistatic coupling of the two electric moments, for magnetic dipole emitters the gap introduced an additional minus sign in the coupling term at certain spatial positions. This can also be interpreted by the magnetic field induced by the electric dipole moment of the SRR. Furthermore, we demonstrated that increasing the distance between the emitter and the SRR flips the spectra on the frequency axis.

Although the fundamental plasmon mode of the SRR is a bright mode, the nonradiative decay channel is still dominant, leading to strong quenching. By using more sophisticated nanoantennas, such as dolmen structures [36–39] or oligomers [40,41], where the coupling between the bright electric dipole resonance and the dark magnetic mode can be selectively tuned, it will be possible to

optimize the structure for better coupling to the magnetic dipoles as well as to the radiative far field.

We would like to thank Rashid Zia for very helpful discussions. We would also like to thank the DFG, the BMBF, the Baden-Württemberg-Stiftung, the ERC (Advanced Grant COMPLEXPLAS) as well as the MWK Baden-Württemberg for financial support.

*s.hein@pi4.uni-stuttgart.de
†h.giessen@pi4.uni-stuttgart.de

[1] O. Jitrik and C. F. Bunge, J. Phys. Chem. Ref. Data **33**, 1059 (2004).
[2] L. Reekie, I. Jauncey, S. Poole, and D. Payne, Electron. Lett. **23**, 1076 (1987).
[3] E. M. Purcell, Phys. Rev. **69**, 681 (1946).
[4] A. Kwadrin and A. F. Koenderink, Phys. Rev. B **87**, 125123 (2013).
[5] S. Karaveli and R. Zia, Phys. Rev. Lett. **106**, 193004 (2011).
[6] T. H. Taminiau, Z. Karaveli, N. F. van Hulst, and R. Zia, Nat. Commun. **3**, 979 (2012).
[7] L. A. Blanco and F. J. Garcia de Abajo, Phys. Rev. B **69**, 205414 (2004).
[8] P. Anger, P. Bharadwaj, and L. Novotny, Phys. Rev. Lett. **96**, 113002 (2006).
[9] L. Rogobete, F. Kaminski, M. Agio, and V. Sandoghdar, Opt. Lett. **32**, 1623 (2007).
[10] G. Colas des Francs, G. Sanchez-Mosteiro, M. Ujue-Gonzalez, L. Markey, N. F. van Hulst, and A. Dereux, J. Microsc. **229**, 210 (2008).
[11] V. Giannini, J. A. Sánchez-Gil, O. L. Muskens, and J. Gómez-Rivas, J. Opt. Soc. Am. B **26**, 1569 (2009).
[12] A. M. Kern and O. J. F. Martin, Nano Lett. **11**, 482 (2011).
[13] M. Frimmer, T. Coenen, and A. F. Koenderink, Phys. Rev. Lett. **108**, 077404 (2012).
[14] S. V. Lobanov, T. Weiss, D. Dregely, H. Giessen, N. A. Gippius, and S. G. Tikhodeev, Phys. Rev. B **85**, 155137 (2012).
[15] T. Feng, Y. Zhou, D. Liu, and J. Li, Opt. Lett. **36**, 2369 (2011).
[16] A. M. Kern and O. J. F. Martin, Phys. Rev. A **85**, 022501 (2012).
[17] L. Novotny and N. van Hulst, Nat. Photonics **5**, 83 (2011).
[18] P. Biagioni, J.-S. Huang, and B. Hecht, Rep. Prog. Phys. **75**, 024402 (2012).
[19] V. V. Klimov and V. S. Ketokhov, Laser Phys. **15**, 61 (2005).
[20] B. Rolly, B. Bebey, S. Bidault, B. Stout, and N. Bonod, Phys. Rev. B **85**, 245432 (2012).
[21] M. K. Schmidt, R. Esteban, J. J. Sáenz, I. Suárez-Lacalle, S. Mackowski, and J. Aizpurua, Opt. Express **20**, 13636 (2012).
[22] R. Filter, S. Mühlig, T. Eichelkraut, C. Rockstuhl, and F. Lederer, Phys. Rev. B **86**, 035404 (2012).
[23] L. Novotny and B. Hecht, *Principles of Nano-Optics* (Cambridge University Press, Cambridge, England, 2011), pp. 271–283.
[24] In the case of electric dipoles, one has to replace $\boldsymbol{\mu}$ by $\boldsymbol{p}$ and use the electric Green's function instead.
[25] A. F. Koenderink, Opt. Lett. **35**, 4208 (2010).
[26] M. A. Yurkin and A. G. Hoekstra, J. Quant. Spectrosc. Radiat. Transfer **106**, 558 (2007).
[27] Due to the fact that the outer shell of dipoles takes up a substantial amount of volume, the structure appears to be effectively thinner in our simulations. This leads to a redshift in comparison to highly accurate simulations, however it does not change the spectral shape of the plasmon modes.
[28] V. Myroshnychenko, J. Rodriguez-Fernandez, I. Pastoriza-Santos, A. M. Funston, C. Novo, P. Mulvaney, L. M. Liz-Marzan, and F. J. Garcia de Abajo, Chem. Soc. Rev. **37**, 1792 (2008).
[29] P. B. Johnson and R. W. Christy, Phys. Rev. B **6**, 4370 (1972).
[30] I. Sersic, C. Tuambilangana, T. Kampfrath, and A. F. Koenderink, Phys. Rev. B **83**, 245102 (2011).
[31] M. A. Yurkin and A. G. Hoekstra, J. Quant. Spectrosc. Radiat. Transfer **112**, 2234 (2011).
[32] J. W. Hennel and J. Klinowski, *Topics in Current Chemistry* (Springer, New York, 2005), Chap. 1, pp. 1–14.
[33] P. Bharadwaj and L. Novotny, Opt. Express **15**, 14 266 (2007).
[34] H. Mertens, A. F. Koenderink, and A. Polman, Phys. Rev. B **76**, 115123 (2007).
[35] R. Taubert, R. Ameling, T. Weiss, A. Christ, and H. Giessen, Nano Lett. **11**, 4421 (2011).
[36] S. Zhang, D. A. Genov, Y. Wang, M. Liu, and X. Zhang, Phys. Rev. Lett. **101**, 047401 (2008).
[37] N. Liu, L. Langguth, T. Weiss, J. Kästel, M. Fleischauer, T. Pfau, and H. Giessen, Nat. Mater. **8**, 758 (2009).
[38] N. Verellen, Y. Sonnefraud, H. Sobhani, F. Hao, V. V. Moshchalkov, P. V. Dorpe, P. Nordlander, and S. A. Maier, Nano Lett. **9**, 1663 (2009).
[39] N. Liu, T. Weiss, M. Mesch, L. Langguth, U. Eigenthaler, M. Hirscher, C. Sönnichsen, and H. Giessen, Nano Lett. **10**, 1103 (2010).
[40] M. Hentschel, M. Saliba, R. Vogelgesang, H. Giessen, A. P. Alivisatos, and N. Liu, Nano Lett. **10**, 2721 (2010).
[41] J. B. Lassiter, H. Sobhani, J. A. Fan, J. Kundu, F. Capasso, P. Nordlander, and N. J. Halas, Nano Lett. **10**, 3184 (2010).